

# Solid-state $^{13}\text{C}$ nuclear magnetic resonance spectroscopy of ethylene/vinyl alcohol copolymers: morphological partitioning of hydroxyls

D. L. VanderHart\*

*Polymers Division, National Institute of Standards and Technology, Gaithersburg, MD 20899, USA*

and Stephanie Simmons

*Program in Polymer Science and Technology, Department of Chemical Engineering, Massachusetts Institute of Technology, Cambridge, MA 02139, USA*

and J. W. Gilman

*Fire Science Division, National Institute of Standards and Technology, Gaithersburg, MD 20899, USA*

*(Received 24 February 1995; revised 13 March 1995)*

Cross-polarization/magic angle spinning (CP/MAS)  $^{13}\text{C}$  nuclear magnetic resonance (n.m.r.) spectra of several random ethylene (E)/vinyl alcohol (VOH) copolymers, including both homopolymers, have been obtained. Contributions to these spectra arising from the crystalline and non-crystalline regions of these materials have been isolated and from these spectra the average concentrations of the comonomers in the crystalline phase is determined. For melt-crystallized samples, the composition of the crystals is very close to stoichiometric, thereby supporting the notion, for example, that VOH and E residues may act as interstitial- or vacancy-type defects in the polyethylene or poly(vinyl alcohol) lattices, respectively. Assuming the validity of a previously proposed assignment scheme for the methine multiplets visible in the E-rich composition range, we conclude that there is no significant discrimination against VOH–VOH sequences in the crystalline regions. In one sample containing 18 mol% VOH, it was shown that simultaneous with VOH incorporation, other ‘defects’ were, within the signal-to-noise, rejected from the crystalline regions. These defects, mainly short-chain branches totalling about 8 branch points per 1000 main-chain carbons, included ethyl and butyl-plus-longer branches (from polymerization side reactions) as well as acetate branches (from incomplete hydrolysis of the precursor copolymer). In contrast to the melt-crystallized samples, copolymers precipitated from isopropanol show a slight bias in their crystalline regions towards a more E-rich composition, presumably because E-rich stems are more available at the time of crystallization via their decreased solubility in this solvent. Finally, a few observations are made regarding the PVOH homopolymer in the dry and slightly hydrated state. Spectral changes are not entirely consistent with trends reported in the literature. Thus, a question is raised whether possible variations in molecular mobility within the PVOH crystalline regions can give rise to systematic differences in crystalline-phase spectra isolated by different  $^{13}\text{C}$  n.m.r. spectroscopic methods.

**(Keywords: solid-state n.m.r.; random copolymers; melt crystallization)**

## INTRODUCTION

Early studies<sup>1,2</sup> investigating the crystallinity of a random copolymer of ethylene (E) and vinyl alcohol (VOH) reported that both E and VOH residues are incorporated into the crystalline regions, thus forming ‘mixed crystals’. Other investigators<sup>3–9</sup> employing thermal analysis, X-ray diffraction, and  $^{13}\text{C}$  n.m.r. spectroscopy have argued for similar conclusions and have even proposed the existence of a pseudohexagonal crystal structure at intermediate E and VOH compositions<sup>5</sup>.

While there is little doubt that both kinds of residues are incorporated, some ambiguity remains regarding the morphological partitioning of the comonomers between the crystalline (CR) and non-crystalline (NC) regions. Matsumoto and coworkers<sup>4,5</sup> found evidence that lower-than-stoichiometric VOH contents exist in CR regions over a certain range of composition including 36 mol% VOH. In other words, there may be some tendency to reject the VOH comonomer when the prevailing crystal lattice is not the poly(vinyl alcohol) (PVOH) lattice. In this paper, we make use of a solid-state  $^{13}\text{C}$  n.m.r. spectroscopic technique<sup>10</sup> which allows one to isolate the spectrum of the CR regions and to assess the level of VOH residues in these regions.

\* To whom correspondence should be addressed

In previous work we have measured the partitioning of rather dilute defects in the polyethylene lattice<sup>10,11</sup>. We have shown that, to varying degrees, both vinyl and methyl chain ends as well as methyl and ethyl side branches show partitioning, i.e. show a preference for the non-crystalline regions. Thus, it was intriguing for us to consider whether, at lower concentrations, the VOH residues go into the polyethylene lattice stoichiometrically, i.e. whether there is *no* partitioning in EVOH copolymers. In principle, understanding the strength of partitioning can be useful in terms of controlling the morphology and mechanical properties of a copolymer. If partitioning exists, there are at least two ways in which this control might be exercised. First, crystal size and crystallinity can be controlled by changing the concentration of defects. (In EVOH, there is a modest dependence of crystallinity on VOH concentration<sup>4</sup>.) Secondly, creep properties in drawn materials can be altered<sup>12</sup> via the introduction of groups which are excluded from the crystalline regions (assuming that an important mechanism for creep is the transport of chain segments through the crystalline regions). In this regard, EVOH copolymers present an interesting challenge since the 'defects' in these materials are not limited to the minor copolymer species. In addition, there are short chain branches and residual acetate branches arising from the fact that the EVOH copolymers are saponified, although perhaps not completely, from ethylene/vinyl acetate copolymers. The latter materials are polymerized in a manner similar to low-density polyethylene, which, in turn, is known to contain many short chain branches<sup>13</sup>. Therefore, even if there is no partitioning of the VOH residues, it is of interest to know whether there is a simultaneous partitioning of these other defects.

The major objective of this paper is to evaluate the VOH incorporation in the CR regions for six-different melt-crystallized EVOH copolymers. Therefore, via the required isolation of spectra associated with CR regions, we can comment briefly both on the incorporation of short branches into the CR regions and on the dependence of the comonomer concentration on crystallization history.

We also present some spectral observations regarding the methine resonance for both a dry and slightly hydrated sample of the PVOH homopolymer. The methine resonance profile is a triplet whose component intensities are correlated with triad tacticity; nevertheless, component intensities depart from the actual triad tacticities<sup>14</sup>. Different explanations<sup>9,14</sup> have been offered to explain this departure; moreover, these intensities are also influenced by the presence of water<sup>15</sup>. The comments we will offer regarding PVOH deal primarily with a mildly hydrated PVOH sample where the separation of signals from the CR regions yields results which run counter, in some respects, to previously published work.

## EXPERIMENTAL

### Materials

EVOH random copolymers having a wide range of composition were studied; most of these were available commercially. Others were prepared from ethylene/vinyl acetate copolymers; details of these preparations

are included below. VOH and E polymers were also studied.

Low-density polyethylene (LDPE) is the ethylene homopolymer most closely related to the EVOH copolymers by virtue of the similarity in polymerization conditions. The LDPE used here was the former standard reference material, SRM 1476, of the National Institute of Standards and Technology (NIST) ( $M_n = 20\,000$ ,  $M_w = 100\,000$ )<sup>16</sup>. The PVOH used in this work was Elvanol<sup>®</sup> HV (Du Pont)<sup>17</sup>. Du Pont also supplied us with the following additional information about this material:  $M_n = 107\,500$ ;  $M_w = 199\,000$ ; triad tacticity,  $mm = 0.20$ ,  $mr = 0.50$ , and  $rr = 0.30$  ( $m = \text{meso}$  and  $r = \text{racemic}$  in dyad nomenclature).

The EVOH copolymers with mole fractions of 0.10, 0.18 ( $M_n = 36\,000$ ,  $M_w = 84\,000$ ), 0.56 ( $M_n = 44\,000$ ,  $M_w = 97\,000$ ) and 0.68 VOH ( $M_n = 53\,000$ ,  $M_w = 119\,000$ ) were obtained from Polysciences, Inc. The foregoing molecular weights were measured by conventional gel permeation chromatography (g.p.c.) using dimethylacetamide containing 0.2% LiBr at 90°C as the mobile phase. Values are referenced to a polystyrene standard. The sample with 10 mol% VOH was not measured because of solubility problems with this solvent. Compositions were checked using solution proton n.m.r. spectroscopy.

Poly(ethylene-vinyl alcohol) copolymers, containing 14 and 21 mol% VOH, were prepared in our laboratory from poly(ethylene-vinyl acetate) (PVAc) copolymers according to a published method<sup>18</sup>. PVAc (4.0 g, 0.015 mol, 33 wt% vinyl acetate, beads from Scientific Polymer Products,  $M_w = 155\,000$ , lot No. 4, 3/17/94) was added to a solution of toluene (100 ml, ACS reagent grade), benzene (100 ml, HPLC grade), isopropanol (100 ml, AR grade) and KOH (4.14 g, 0.08 mol, 5 equivalents per vinyl acetate equivalent) at reflux (80°C) under N<sub>2</sub>. Reflux was maintained for 2 h. The solution (light yellow) became cloudy as it cooled to ambient temperature in a water bath. Isopropanol (180 ml) was added with rapid stirring to further precipitate the EVOH copolymer product. The white powdery solid was collected and washed with isopropanol (50 ml), isopropanol/H<sub>2</sub>O (1/1, 100 ml), methanol/H<sub>2</sub>O (1/1, 100 ml), and methanol (100 ml). The product was dried *in vacuo* (70°C) to a constant weight (3.10 g, 92% yield).

PVAc copolymer (4.0 g, 0.021 mol, 45 wt% vinyl acetate, beads from Scientific Polymer Products,  $M_w = 260\,000$ , lot No. 1, 3/17/94) was added to a solution of toluene (100 ml, ACS reagent grade), benzene (100 ml, HPLC grade), isopropanol (100 ml, AR grade) and KOH (5.5 g, 0.1 mol, 5 equivalents per vinyl acetate equivalent) at reflux (80°C) under N<sub>2</sub>. Reflux was maintained for 3.5 h. The solution (light yellow) did not become cloudy as it cooled to ambient temperature in a water bath. Isopropanol (500 ml) was added with rapid stirring to precipitate the EVOH copolymer product. The precipitation continued slowly over a 12 h period. The white powdery solid was collected via centrifugation and filtration and was washed with isopropanol/H<sub>2</sub>O (1/1, 150 ml), methanol/H<sub>2</sub>O (1/1, 150 ml), and methanol (100 ml). The product was dried *in vacuo* (25°C) to a constant weight (3.10 g, 99% yield).

Judging by the strength of the carbonyl signal of the acetate moiety, the saponification process converted

greater than 99% of the acetates to hydroxyls in both of the above samples. In contrast, the copolymers obtained from Polysciences with 10 and 18 mol% VOH showed a degree of saponification in the 95–96% range. We did not similarly characterize the remaining EVOH samples.

Materials in their 'as-received' condition were used without any attempt to dry them. During our study we became concerned that the presence of water might influence our results. The direct observation of 200 MHz solid-state proton n.m.r. spectra from Bloch-decay signals acquired on a Bruker CXP200 spectrometer showed that water contents in the as-received materials were all less than 0.8 wt%. An exception to this was the PVOH sample which had 6 wt% water; this sample will be designated as PVOH-6. Melt-crystallized samples (not including PVOH because of thermal instability issues) were prepared by melting under vacuum at temperatures at least 20°C above their measured differential scanning calorimetry (d.s.c.) melting points and then cooling through the crystallization temperatures at rates of  $\sim 0.8^\circ\text{C min}^{-1}$ . The measured melting points in  $^\circ\text{C}$  (with the corresponding mole fractions of VOH) are: 99(0.10), 109(0.18), 165(0.56), 182(0.68) and 228(1.00). Melting under vacuum dries the samples and these samples were used immediately so as to avoid any significant moisture pick-up.

A second PVOH sample (PVOH-0) was vacuum dried at 100°C for 16 h and subsequently analysed. Other authors have reported significant changes in PVOH  $^{13}\text{C}$  n.m.r. spectra as a function of the degree of hydration<sup>15</sup>. Copolymer spectra are less influenced by water; this latter fact is probably a result of the copolymer's reduced affinity for water. One as-received EVOH sample was dried at ambient temperature in vacuum in order to verify the insensitivity of the partitioning to the presence of the small amount of water. This dried sample contained less than 0.1% water, according to its Bloch-decay proton lineshape.

### Nomenclature

Nomenclature for the EVOH copolymers adopts the following rules: the first part of the designation refers to the mol% VOH; secondly, suffixes are added (MC = 'melt-crystallized', N = 'annealed', D = dried in vacuum at ambient temperature) in sequence, depending on further treatment. Thus, for example, V18-MC-N refers to a sample, which has been melt-crystallized and then annealed, having 18 mol% VOH.

### Spectroscopy

$^{13}\text{C}$  n.m.r. spectra were acquired in a standard way<sup>19</sup> on a non-commercial spectrometer operating at 2.35 T (25.2 MHz). The probe is also non-commercial, but it incorporates a 7-mm magic angle spinning (MAS) rotor and stator system manufactured by Doty Scientific, Inc. The MAS frequencies were 3.1–3.2 kHz, unless otherwise noted; r.f. levels for cross-polarization (CP) and decoupling correspond to nutation frequencies of 66 kHz for protons and 69 kHz for  $^{13}\text{C}$  nuclei. The CP time was 1 ms for all spectra. Variable spin-locking (SL) times, usually 1  $\mu\text{s}$  and 5 ms, preceded the CP step and the associated spectra were those from which morphological-component spectra were generated. SL times were changed every 80 scans in order to minimize the influence of any spectral drift when the SL data were acquired.

Generally, 5000–15 000 scans were taken in order to generate adequate signal-to-noise for isolating the component spectra. Delays between acquisitions ranged from 3 to 5 s, depending on the longitudinal proton relaxation times,  $T_{1\rho}^{\text{H}}$ .

### Method for isolating component spectra

The method for isolating the spectrum of the CR region from that of the NC region has been discussed previously<sup>10</sup>. The key assumptions behind the method are as follows: (a) during the 1 ms of CP time, proton spin diffusion<sup>20</sup> is facile enough to maintain a uniform polarization per proton spin over distances characteristic of the E or VOH residues, (b) the intrinsic rotating frame relaxation time,  $T_{1\rho}^{\text{H}}$ , is different for protons in the CR and NC regions and the regions are large enough, relative to spin diffusion rates, so that average proton polarization gradients between these regions develop during spin locking, (c) the polymer morphology is two-phase, CR and NC, and (d) resonances in the CR may be distinguished from those in the NC by the superior resolution characterizing the former, i.e. disorder in the NC regions causes excess line broadening owing to more motional broadening as well as a variability in conformation and interchain packing<sup>21,22</sup>. Proceeding on the basis of these assumptions, one isolates the spectra of the CR and NC regions by taking linear combinations of spectra with different spin locking times. Figure 1 illustrates this method for the V18-MC-N sample. The two upper spectra correspond to 1  $\mu\text{s}$  and 5 ms SL times with the latter spectrum vertically amplified to allow better lineshape comparison. Owing to a shorter  $T_{1\rho}^{\text{H}}$  in the NC regions compared to the CR regions, the spectrum at 5 ms SL time is relatively richer in the CR component than the spectrum at 1  $\mu\text{s}$  SL time. Hence,

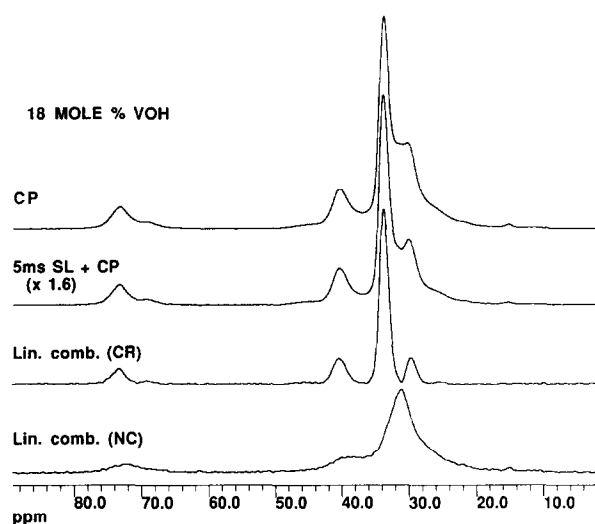


**Figure 1** 25.2 MHz CP/MAS  $^{13}\text{C}$  n.m.r. spectra of sample V18-MC-N, a melt-crystallized and annealed EVOH copolymer with 18 mol% VOH residues. These spectra illustrate the isolation of lineshapes corresponding to the crystalline (CR) and non-crystalline (NC) components of this sample. The top two spectra are experimental and both derive from a 1 ms cross-polarization (CP) time; conditions differ in the spin-locking times which precede CP, namely 1  $\mu\text{s}$  for the 'CP' spectrum and 5 ms for the other. These spectra represent different mixtures of the signals from the CR and NC regions. The CR and NC lineshapes are linear combinations of the top two spectra; the sum of these lineshapes in this figure is the CP spectrum. The MAS frequency in this figure is 3.2 kHz

appropriate linear combinations of these two spectra yield the CR and NC lineshapes given in Figure 1. The criterion for selecting the linear combination for the CR spectrum is that the resolution of the spectrum be maximized while avoiding negative-going intensities. Since the NC spectrum has generally broader resonances, there are usually spectral regions where only the NC intensities contribute; hence, defining a linear combination where these unique regions are nulled offers a relatively unambiguous criterion for defining the CR spectrum. Defining the linear combination corresponding to the NC spectrum is a more subjective activity, especially when the NC resonances for each carbon span the spectral range of the CR resonances, as they do in the EVOH case. (We shall use the terms 'CR resonances' and 'NC resonances' to refer to resonances in the corresponding spectra of the CR and NC components.) Given this overlap of the CR and NC resonances, the NC spectrum, i.e. that linear combination in which the CR resonances are nulled, is a spectrum where all resonances are still positive. Thus, the subjective aspect is that one must judge at what point the minimum amount of sharper features appear, either as 'bumps' or 'depressions' in the spectra. The choice of this NC linear combination is not as accurately made relative to the choice for the CR spectrum, yet one can usually find a reasonable lineshape for the NC spectrum, as illustrated in Figure 1.

The important implication of the foregoing remarks is that one can isolate the CR spectrum with considerable confidence and thereby make a reasonably accurate determination of the concentration of VOH residues in the CR; however, the uncertainty in the determination of the NC spectrum shows up primarily as an uncertainty in the apparent CR fraction,  $f_c^*$ , associated with the 1  $\mu$ s SL spectrum.

We pause to make a few comments about the determination of crystallinity. The 1  $\mu$ s SL spectrum is generally regarded as a good approximation to the undistorted relative intensities for both the CR and the NC fractions. However, during the 1 ms of CP time, there is a preferential  $T_{1\rho}^H$  decay of the proton polarization in the NC regions. One can make an approximate correction for this effect by estimating the intrinsic  $T_{1\rho}^H$ s in each region from the fractional decay over the first 5 ms of SL time. Then, using these estimated  $T_{1\rho}^H$  values, one can generate corrected crystallinity values,  $f_c$ , which account for the unequal decay over the 1 ms of CP time. For the EVOH samples, these corrections were small, i.e. the  $f_c$  values were 0.93–0.95 times the  $f_c^*$  values. A final comment on the determination of crystallinity in this way is that corrections related to the influences of possibly different CP efficiencies or different pathways for relaxation to the lattice during CP for the signals from the two regions have not been considered. Sometimes these are not negligible<sup>10</sup>. Hence, since accounting for these effects usually results in a reduction in crystallinity, the  $f_c$  values should be considered as upper limits to crystallinity.

## RESULTS

General spectral assignments in Figure 1 are as follows: the methine carbons appear in the 64–76 ppm range with a maximum at 73 ppm and a shoulder near 69 ppm (the

apparent mole fraction of VOH residues in any of these spectra is simply twice the fractional intensity of this methine region, relative to the total intensity); all other interior-chain carbons are methylene carbons and, in the CR spectrum, lines at 40.4, 29.5 and 33.8 ppm correspond, respectively, to carbons that are  $\alpha$ ,  $\beta$  and further-than- $\beta$  from a single CHOH carbon<sup>23</sup>. If the VOH residues were infinitely dilute in the chain, the  $\alpha$  and  $\beta$  resonances would be twice the intensity of the methine region; the fact that the  $\alpha$  and  $\beta$  peaks have somewhat smaller relative intensities in the CR spectrum (with the  $\beta$  intensity also smaller than the  $\alpha$  intensity) is expected based on the random character of the monomer sequence and the increased chance of short-range pairs of VOH residues (*versus* isolated VOH residues) as the mol% VOH increases. In the NC spectrum of Figure 1, the peak at 31.0 ppm is dominated by the NC ethylene residues; this peak coincides with the NC peak of PE<sup>24</sup>.

Figure 2 shows vertically expanded portions of three spectra analogous to those of Figure 1; the difference is that the spinning speed was increased to avoid sideband overlap in the carbonyl region (171 ppm) where residual acetate groups can be detected. Lineshape differences between the CR and NC contributions to the 1- $\mu$ s-SL CP spectrum are highlighted for the carbonyl region, the methine region and the methyl region. In the methine region, distinct CR resonances at 73.2 and 69.0 ppm are visible. The implied level of VOH incorporation in the CR region is  $0.184 \pm 0.008$ , i.e. very close to the overall mole fraction of  $0.178 \pm 0.005$ . The NC profile shows a peak at 72.5 ppm with an asymmetric tailing towards high field; most of the high-field shoulder of the CP spectrum is, therefore, of NC origin.

In Figure 2 the methyl region is shown together with the methyl region of LDPE. The methyl resonance at 15.0 ppm arises from linear chain segments of 4 or more carbons in length; for LDPE, this resonance is

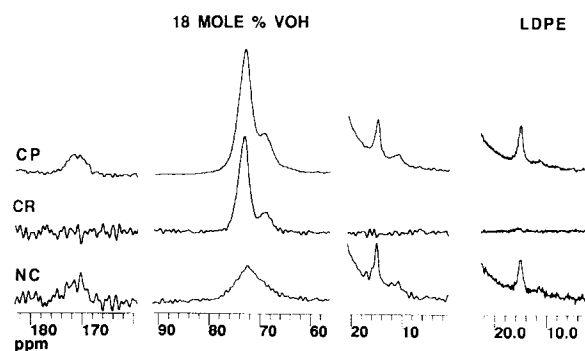


**Figure 2** Portions of spectra illustrating the partitioning of branches and VOH 'defects' between the CR and NC regions for the V18-MC-N and the LDPE samples. Labels are the same as those used in Figure 1; the MAS frequency is 4 kHz, in order to avoid interferences from spinning sidebands. For the V18-MC-N spectra, vertical amplification factors vary for each region:  $\times 4$ ,  $\times 1$  and  $\times 2$  for the residual-acetate-carbonyl (171 ppm) region, the VOH-methine (66–77 ppm) region and the methyl (10–20 ppm) region, respectively. Methyl signals, dominated by butyl branches at 15 ppm and by ethyl branches at 11 ppm are visible. The spectra show that, within the signal-to-noise, butyl and ethyl branches are excluded from the CR regions in both the copolymer and LDPE. This same condition prevails for the residual acetate groups while, simultaneously, the VOH residues are incorporated into the CR region in large numbers. Note that the fractional intensity of the upfield wing of the methine resonance is significantly reduced in the CR lineshape relative to the CP spectrum

dominated by the methyls of butyl branches<sup>13</sup>. We will refer to this resonance as the C4+ resonance and to the branches as C4+ branches. A weaker feature near 11 ppm is the methyl resonance of ethyl branches<sup>13</sup>. Within the signal-to-noise, these branches, whose apparent concentration in the 1  $\mu$ s SL spectrum is, respectively, about 3 and 1 per 1000 carbons, are excluded from the CR regions of the LDPE. Only a very weak resonance at about 15.5 ppm is visible in the CR spectrum, and these latter methyls are assigned to long chain ends in the CR region, consistent with earlier determinations<sup>10</sup> on linear PE samples. Since the precursor ethylene/vinyl acetate copolymer for these EVOH copolymers is polymerized similarly to LDPE, it is reasonable to expect that the 15.0 ppm peak in the V18-N sample is also dominated by methyls on butyl branches. The ethyl methyl resonance is also discernible. The apparent concentration of such methyls is 3.5 and 1.5 per 1000 carbons for the 15.0 and 11 ppm resonances, respectively. The main point to be illustrated in Figure 2 is that within the signal-to-noise levels, these C4+ and ethyl branches are excluded from the CR regions, in spite of the simultaneous, substantial incorporation of VOH residues into the CR. The carbonyl region indicates a similar situation for the acetate group. The implied concentration of acetate groups is about 4 per 1000 carbon atoms in the CP spectrum.

Figures 3 and 4 show, respectively, 1- $\mu$ s-SL CP and CR spectra pertaining to melt-crystallized samples of the 6 EVOH copolymers along with LDPE and PVOH-6. Table 1 lists the values for vinyl alcohol composition (in mol%), as given by the supplier ( $\chi_{VS}$ ), as tabulated from the 1- $\mu$ s-SL CP spectra ( $\chi_{VCP}$ ), and as determined for the CR spectra ( $\chi_{VC}$ ). Also included are the  $T_{1\rho}^H$ -corrected crystallinities,  $f_c$ , determined from the n.m.r. spectroscopic data, along with the crystallinities,  $f_{cX}$ , determined from X-ray powder diffraction patterns<sup>25</sup> on selected samples. The crystallinities determined by the two methods are in reasonable agreement; moreover, they are in the same

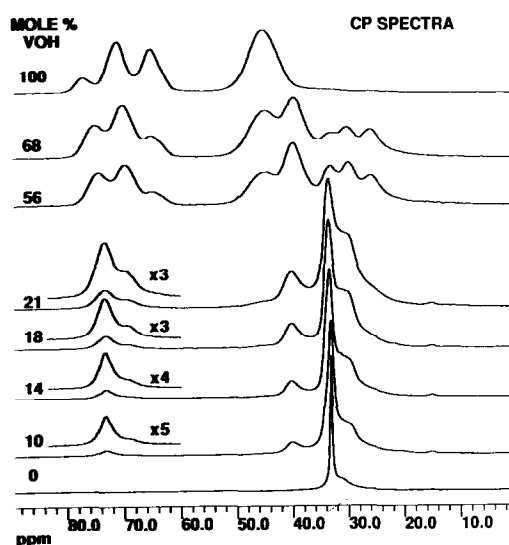


**Figure 3** Collection of CP spectra obtained for dry, melt-crystallized samples with compositions as indicated; the PVOH homopolymer sample is the exception since it is not melt crystallized and contains ~ 6 wt% water. Vertically amplified methine regions are also shown; spectra are not normalized in total intensity

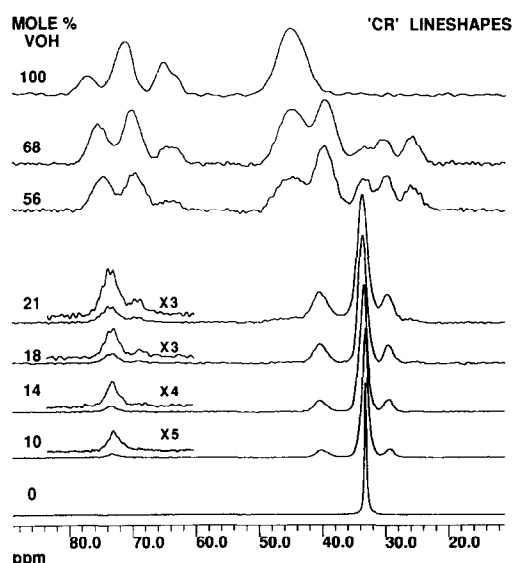


**Figure 4** CR lineshapes corresponding to the spectra of Figure 3; note the general enhancement of the downfield multiplet component of the methine resonances in these spectra relative to the CP spectra of Figure 3

range as those reported by others<sup>4,26</sup>. As implied earlier, crystallinities are expected to be strongly dependent on the branch content for the E-rich copolymers. While it is not our intent to focus on the role of short-chain branching in determining crystallinity, we will simply make one observation. The lower crystallinity of the V10 samples, relative to those of the V18 samples, is not determined by the short-chain branching levels which we can monitor, namely those of the ethyl, C4+ and acetate branches. In the V10 sample, the concentrations of C4+ and ethyl branches are, within 20%, the same as those found in the V18 sample, while the acetate concentration in V10 is only 50–60% of that found in the V18 sample. Thus, unless the distribution of branches associated with the C4+ resonance is different in the two materials, there must be another explanation for the lower relative crystallinities of the V10 samples.

The influence of annealing near  $T_m$ , both before and after melt crystallization, was examined for the V10 and V18 samples. It was found that the level of VOH incorporation into the CR regions as well as the CP and CR lineshapes closely approximated what was found for the melt-crystallized samples. We did not conduct annealing studies on the V56 and V68 samples owing to the very similar  $\chi_{VC}$  values obtained for the pairs of as-received and melt-crystallized samples. Therefore, we view the spectra shown in Figure 4 as reporting, to a good approximation, thermodynamically equilibrated partitioning into the CR regions via crystallization from the melt state.

The values of  $\chi_{VC}$  given in Table 1 were found to be sensitive to the sample preparation conditions. Significant differences, particularly in the CR spectra for the V18 and V21 samples, were observed in going from the untreated, as-received samples to the melt-crystallized (or annealed) conditions. In Figure 5 CR spectra for these two samples, normalized pairwise to the same VOH-related resonance intensities, are shown for the untreated and melt-crystallized conditions. These pairs of spectra are overlaid along with the difference spectra.

**Table 1** Mol% VOH values<sup>a</sup>, as given by the supplier ( $\chi_{VS}$ ), as obtained from the 1  $\mu$ s SL spectra ( $\chi_{VCP}$ ), and as obtained from the CR spectrum ( $\chi_{VC}$ ), along with the n.m.r. crystallinities<sup>b</sup> ( $f_c$ ), X-ray crystallinities<sup>b</sup> ( $f_{cX}$ ), and annealing parameters for the homopolymers and EVOH copolymers; estimated maximum departures from the given values, in units of the last decimal place, are shown in parentheses

Sample <sup>c</sup>	Annealing parameters		VOH content (mol%)			Crystallinity	
	<i>T</i> (°C)	<i>t</i> (h)	$\chi_{VS}$	$\chi_{VCP}$	$\chi_{VC}$	$f_c$	$f_{cX}$
LDPE	—	—	—	—	—	0.43 (3)	—
V10	—	—	10.0 (5)	10.1 (5)	8.0 (10)	0.31 (3)	0.3 (3)
V10-MC	—	—	10.0 (5)	9.2 (6)	9.6 (10)	0.28 (3)	—
V10-MC-N	94	34	10.0 (5)	9.2 (5)	10.2 (10)	0.28 (3)	—
V10-N	92	23	10.0 (5)	9.5 (4)	9.8 (6)	0.28 (3)	—
V14	—	—	13.8 (5)	12.6 (5)	11.0 (10)	0.41 (4)	—
V14-MC	—	—	13.8 (5)	14.0 (5)	13.2 (10)	0.34 (4)	—
V18	—	—	17.8 (5)	18.1 (5)	14.2 (10)	0.42 (4)	0.38 (2)
V18-MC	—	—	17.8 (5)	18.0 (5)	19.1 (10)	0.38 (4)	—
V18-MC-N	94	34	17.8 (5)	18.0 (4)	18.4 (8)	0.50 (4)	—
V18-N	94	36	17.8 (5)	17.8 (5)	19.1 (10)	0.44 (4)	—
V21	—	—	21.0 (5)	21.7 (6)	18.1 (10)	0.39 (4)	—
V21-MC	—	—	21.0 (5)	21.8 (6)	24.0 (12)	0.34 (5)	—
V21-D	—	—	21.0 (5)	21.4 (6)	18.7 (8)	0.41 (4)	—
V56	—	—	56 (1)	57.8 (15)	63 (2)	0.47 (6)	0.42 (4)
V56-MC	—	—	56 (1)	56.8 (15)	61 (2)	0.46 (5)	—
V68	—	—	68 (1)	67.8 (15)	71 (3)	0.46 (7)	0.47 (4)
V68-MC	—	—	68 (1)	67.0 (15)	70 (2)	0.37 (7)	—
PVOH-6	—	—	100	100	100	0.53 (7)	0.48 (3)

<sup>a</sup>  $\chi_{VCP}$  and  $\chi_{VC}$  are determined by integration: mol% =  $200 \times I(\text{methine})/I(\text{total})$ , where  $I$  is the integrated intensity

<sup>b</sup> The CR fraction,  $f_c$ , is based on the relative contributions to the 1  $\mu$ s SL spectrum of the CR and NC components. A correction for differing  $T_{1\rho}$  behaviour in these regions during the 1 ms CP time has also been made based on the component decay rates between 1  $\mu$ s and 5 ms SL times. The crystalline fraction,  $f_{cX}$ , is determined from the X-ray powder pattern

<sup>c</sup> Numerical value is the mol% ethylene content; no suffix means 'as received'; MC = melt crystallized; N = annealed; D = dried in vacuum at ambient temperature; the suffix order is chronological

The significant positive intensities in the 33–35 ppm region of the difference spectra indicate that for each untreated sample, there are fewer VOH residues in the CR regions, relative to the corresponding melt-crystal-

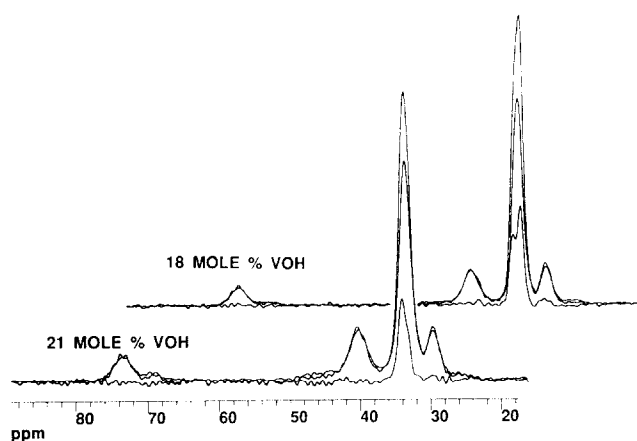


**Figure 5** Comparison of the CR lineshapes, normalized to the same VOH-related intensities, for as-received versus melt-crystallized EVOH samples of the V18 and V21 copolymers. Each pair of lineshapes includes the corresponding difference spectrum. Principal differences occur in the ethylene region (33–34 ppm) where the stronger intensities from the as-received samples indicate crystal compositions richer in ethylene residues. The shape of the difference spectra in the ethylene region may point to regions with monoclinic and orthorhombic PE lattices in the as-received samples

lized samples. Evidently, there is something about the formation of the CR phase in the untreated samples which favours incorporation of the E residues at a level higher than that found after melt crystallization and/or annealing. Incidentally, the lineshape differences of Figure 5 cannot be explained on the basis of the small change in water content between the as-received and melt-crystallized samples. Ambient-temperature drying of the V21 sample resulted in a CR lineshape very similar to that corresponding to the as-received sample, and, within experimental error, the same partitioning values (see the V21-D data shown in Table 1).

We propose the following hypothesis to explain the uniquely lower degree of VOH incorporation in the untreated V21 sample relative to the melt-crystallized (and/or annealed) samples (we do not know the history of the as-received V18 sample). For the V21 sample, crystallization was initiated by the addition of isopropanol. The less-soluble chain segments in isopropanol are those richer in E residues; hence, these segments condense first with the result that the CR composition holds a bias towards higher E values relative to the situation when crystallization occurs from the melt. In addition, since crystallization occurred at ambient temperature, well below<sup>4</sup> the  $T_g$  of  $\sim 48^\circ\text{C}$ , there was little opportunity for subsequent changes in crystal composition.

The difference spectra shown in Figure 5 exhibit either

a doublet (V18) or asymmetric shape (V21) in the ethylene region from 32 to 35 ppm as though there might be two unresolved resonances present. Remembering that we are interpreting a *difference* spectrum where, for example, a doublet can arise from the subtraction of a narrower line from a broader one, it is curious that the doublet position and splitting in the V18 sample coincides closely with what would be expected<sup>27</sup> if both the monoclinic and orthorhombic PE unit cells were present in at least the untreated materials. We do not insist on the interpretation, yet it is plausible.

Relative to the PVOH homopolymer, we call attention only to a few observations regarding the methine region. The multiplet intensities seen there have previously been recognized as sensitive to, but not directly reflecting, the triad tacticity distribution<sup>9,14,28</sup>. One view<sup>14</sup> is that these multiplet intensities in the solid state report the number of intramolecular hydrogen bonds where tacticity permits but does not require such bond formation. Another view<sup>9</sup> is that there are important *intermolecular* steric interactions which result from tacticity variations and these modify the planar zigzag structure of the isolated chain so that a combination of tacticity and chain distortion gives rise to the methine multiplets. In addition to these theories, it is also recognized experimentally that these multiplet intensities show a dependence on temperature and the amount of water present<sup>15</sup>. Most of the comments we offer regarding the PVOH homopolymer relate to the influence of water on the spectra in the methine region. These remarks are offered in the hope that they might play some role in sorting out the true origin of the multiplet intensities. Such knowledge would significantly extend the insights one could obtain from the <sup>13</sup>C n.m.r. spectra.

In Figure 6, 1-μs-SL CP spectra are compared for the dried PVOH-0 sample and the PVOH-6 sample with 6% water. The relative intensities of the three methine peaks, I, II and III, are 13:50:37 and 13:45:42, respectively. The difference spectrum (not shown) reveals that the relative intensity of peak I increases at the expense of the upfield

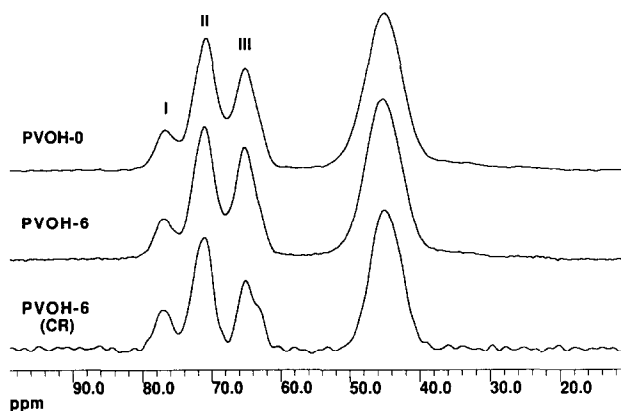


**Figure 6** Comparison of 1-μs SL spectra of poly(vinyl alcohol), normalized to the same total intensity, for the dried PVOH-0 sample and for PVOH-6, i.e. the same sample with 6 wt% water; the spectrum of the CR regions of the PVOH-6 sample is also shown. Note the relative intensity changes in the methine multiplets (62–80 ppm). Multiplet relative intensities for peaks I, II and III are as follows: PVOH-0, 13:50:37; PVOH-6, 13:45:42; PVOH-6 (CR), 17:53:30. The PVOH-6 (CR) ratio approximates to the actual *mm:mr:rr* triad tacticities, i.e. 20:50:30, of this material

side of peak II as water is taken up. Also in Figure 6, the CR spectrum is given for the PVOH-6 sample, and one notes that peak I has an upfield shoulder. This shoulder, associated with the CR phase, has been reported by others<sup>15,29</sup> in samples containing 18% water, in drawn samples, and in dried, solution-crystallized samples; however, the exact origin of this shoulder is not yet defined. Absent in Figure 6 is the CR spectrum of the dried sample because the  $T_{1\rho}^H$  method for separating the CR signal did not work for this sample. Removal of water caused a sufficient lengthening of the  $T_{1\rho}^H$  in the NC region so that both the CR and NC signals decayed at the same rate corresponding to an overall  $T_{1\rho}^H$  of 7.6 ms. Failure of this method for dry PVOH has also been previously reported<sup>15</sup>.

We note a final, rather technical point relative to Figure 6. The contrast in methine multiplet intensities between the CR and 1-μs-SL CP spectra of PVOH-6 appears mainly in the relative decrease of the upfield component in the CR spectrum. In fact, the multiplet intensity ratios in this CR spectrum are very close (17:53:30) to the actual *mm:mr:rr* triad tacticities (20:50:30). This is an agreement not seen before; usually it has been found<sup>15,29</sup> that the relative intensity of peak III is enhanced in the CR spectrum relative to the NC spectrum, with the result that the triad tacticities depart considerably from the multiplet intensities. If agreement between these intensities and triad tacticities were a general result, independent, say, of the presence of water or the thermal history of the sample, then it would have interesting implications relative to our understanding, for example, of the correspondence between strong intramolecular hydrogen bonding and tacticity in the CR regions<sup>14</sup>. The fact that the triad tacticities of PVOH-6 agree so closely with the multiplet intensities may well be a result of differing thermal histories (the history of our sample is unknown to us). On the other hand, this difference may be a commentary on the methods used for isolating the CR spectrum. In previous work<sup>15,29</sup>, the CR spectrum was isolated on the basis of  $T_1^C$  differences, rather than  $T_{1\rho}^H$  differences, which we have used. The physics of the methods are different principally because of the much more facile spin diffusion of protons *versus* <sup>13</sup>C nuclei. Thus, for example, if tacticity variations or variations in hydrogen-bonding patterns resulted in a non-uniformity of mobility on a local monomer scale within the CR phase, one could conceivably generate differences in the CR spectra obtained via the two methods. Moreover, the  $T_{1\rho}^H$  method would then offer a better chance of separating resonances associated with spatially distinct regions. While we do not insist that this is happening for PVOH, future <sup>13</sup>C n.m.r. spectroscopic studies of PVOH should consider this possibility. We did not pursue this matter with lengthy  $T_1^C$  measurements since the focus of this study is to examine comonomer partitioning.

## DISCUSSION

Matsumoto *et al.*<sup>5</sup> concluded from X-ray diffraction diagrams of EVOH copolymers covering the entire composition range, that up to ~20 mol% VOH, crystals adopted the PE lattice, while above 60 mol% VOH, the PVOH crystal lattice was adopted. In the 20–60 mol% VOH range, an intermediate pseudo-hexagonal lattice



was proposed. We did not have access to materials whose composition was well into this intermediate range, so our partitioning results pertain mostly to the modified PE and PVOH lattices.

The general result seen in *Table 1* relating to partitioning of VOH residues in CR regions of melt-crystallized EVOH copolymers is that  $\chi_{VC} \sim \chi_{VCP} \sim \chi_{VS}$ . In other words, the stoichiometry of the CR regions is very close to the overall stoichiometry. The result for the V21-MC sample is tantalizing from the point of view that  $\chi_{VC}$  is somewhat higher than stoichiometric and one wonders whether the intermediate composition range incorporates such a higher level of VOH residues. In addition, the V56-MC and V68-MC samples show a slight excess VOH content above stoichiometric. When E residues are the minority and when the lattice is the PVOH one, incorporation of the smaller E residue will not require energy to expand the lattice; rather the energetic cost of having an E residue in the lattice is a lowering of possibilities for hydrogen bonding and van der Waals interactions. It is known<sup>4</sup> that the average unit-cell volume diminishes when E is substituted for VOH in the PVOH lattice; in contrast, this volume increases when VOH is substituted for E in the PE lattice. This behaviour is respectively consistent with expectations for vacancy-type and interstitial-type lattice defects<sup>30</sup>.

The methine resonance region in the EVOH copolymers is intriguing since there are definite, minimally-overlapping multiplets which are visible in the CR spectra over most of the range of composition. For the PVOH homopolymer, theories about multiplet assignments have already been outlined. We are only aware of one attempt to assign the solid-state multiplets in the EVOH copolymers<sup>9</sup>. In this latter assignment scheme, both tacticity and composition are postulated to play roles in determining the relative multiplet intensities in solid-state spectra. The assignments are the same as those found in solution, albeit this correspondence is not to be taken for granted, especially for hydrogen-bonding solids<sup>31</sup>, and especially in view of the experience with PVOH where the range of solid-state shifts is about three times the liquid-state range<sup>14</sup>. In the proposed copolymer assignment scheme, for lower VOH contents, the lower-field methine line near 73 ppm is assigned to a combination of (a) isolated VOH residues, (b) the central VOH residue in VOH-VOH-E (includes E-VOH-VOH) sequences where the VOH pair has *meso* dyad tacticity, and (c) the central VOH residue in VOH-VOH-VOH sequences with *mm* triad tacticity. The adjacent line, near 69 ppm, is assigned to the central-VOH-methine carbons both in VOH-VOH-E sequences where the VOH pair has *racemic* dyad tacticity and in VOH-VOH-VOH sequences having *mr* triad tacticity. A third line, arising from VOH-VOH-VOH sequences with *rr* triad tacticity, appears near 65 ppm when the VOH content rises to high enough levels to make the number of VOH blocks of length 3 and higher significant.

If one adopts this assignment scheme, then the relative intensities of the 69 and 73 ppm peaks, distinguishable in the CR spectra of *Figure 4*, ought to give some indication whether VOH blocks of 2 or more are preferentially rejected from the CR regions. In the lower VOH mol% range, these methine component intensities are controlled primarily by VOH-VOH pairs. While the

signal-to-noise in the methine region is only modest, it is found that for the four EVOH copolymers in the range from 0.10 to 0.21 mol% VOH, the upfield methine multiplet at 69 ppm constitutes a percentage close to  $\chi_{VC}$  of the total methine intensity. In order to check whether this experimental result is consistent with expectations, we performed some trial calculations. For such calculations one makes assumptions about both the assignment scheme and the distribution of VOH blocks in the CR region; hence, agreement of calculation and experiment does not verify both assumptions independently. Nevertheless, we performed calculations based on the foregoing assignment scheme and on the tentative assumption that VOH blocks are statistically distributed in the CR regions (i.e. there is no partitioning of blocks). We also presumed that the sequences in our copolymers are completely random, as is found for other EVOH copolymers<sup>23</sup>. A final input parameter in the calculations is the dyad probability,  $P_m$ , for the formation of a *meso*-, as opposed to a *racemic*, dyad for any given VOH-VOH sequence. The value of  $P_m$  is 0.45 in the PVOH homopolymer we have used; moreover, for several copolymers in the range with lower E compositions, the reported<sup>32</sup>  $P_m$  values ranged from 0.47 to 0.54. For our purposes, we assume  $P_m = 0.50$ . From known formulae governing the block-frequency distribution of copolymers<sup>33</sup> we can calculate the percentage,  $C_{69}$ , of the total methine intensity resident in the 69 ppm peak. For the following four measured  $\chi_{VC}$  values for the melt-crystallized samples from *Table 1*, the calculated/experimental  $C_{69}$  values follow in parentheses: 9.6(9.1/11), 13.2(12.3/13), 19.1(17.3/16) and 24.0(21.1/24). Given that the estimated error for the experimental values is about  $\pm 3$ , there is good agreement between the calculated and experimental results. Therefore, within the assumption that the assignments are correct, it appears that VOH blocks of length 2 or more are incorporated into the CR regions in numbers commensurate with statistical availability. On the other hand, if the assignment scheme<sup>9</sup> is in error and if, for example, the 69 ppm peak can be assigned exclusively to all VOH residues in VOH-VOH sequences, then the experimental data would favour a partial rejection, or partitioning, of these sequences in the CR regions. One consideration, which is consistent with the 'statistical incorporation of VOH blocks' (thus providing indirect support for the published<sup>9</sup> assignment scheme), is that we did not see any experimental evidence that  $(\chi_{VC}/\chi_{VS})$  diminished as a function of increasing  $\chi_{VS}$ . The latter trend is expected if there were partial rejection of larger VOH blocks owing to the greater fraction of VOH residues present in these blocks as  $\chi_{VS}$  increases. In this connection, we also refer back to *Figure 2* where one might be tempted to interpret the CR and NC methine resonances in a way that would attribute a larger upfield wing intensity to the NC resonance. Thus one might conclude that partitioning of VOH-VOH blocks does occur. At this point we do not regard this as a serious experimental challenge to the 'statistical incorporation' conclusion because (a) adopting the assignment scheme for CR resonances does not automatically carry over to the NC state and (b) there is insufficient resolution in the NC lineshape to suggest a quantitative analysis of different components.

It is interesting that the OH group shows no important partitioning in the polyethylene CR phase while even



short branches of one<sup>11</sup>, two<sup>10</sup> and four carbons, as well as acetate branches (see Figure 2), show significant partitioning. Even methyl and vinyl chain ends show partitioning<sup>11</sup> (although some of the reasons for chain-end partitioning do not pertain to copolymer residues interior to the chain). The fact that these short-chain branches are still strongly rejected by the CR phase in the copolymers of lower VOH content supports the notion that one can achieve some control of crystallinity and, by implication, the mechanical properties, by controlling the level of short-chain branching<sup>3</sup>. In addition, the fact that there is no hint of partitioning at the lowest VOH content of 10 mol% suggests, qualitatively, that hydrogen-bond formation within the CR phase (where the number of opportunities for hydrogen-bond formation is *not* linear in VOH content) is an insignificant driving force for the incorporation of VOH residues in the CR. The OH groups seem to fit into the lattice at a minimal energetic cost; thus, we would concur with the concept<sup>3</sup> that the OH group in the PE lattice simply behaves as a 'point defect'. Given the lattice expansion which accompanies the incorporation of VOH residues into the PE lattice, one might also classify these VOH residues as interstitial defects. In view of the contrast in partitioning between the OH group and short-chain branches, we expect that an appropriate theory of crystallization in these EVOH copolymers, especially in the range where the PE lattice exists, would incorporate features of theories which assume both exclusion<sup>34</sup> and inclusion<sup>35</sup> of defects.

Finally, it is interesting to us that in the E-rich copolymers, the composition of the CR regions is a function of crystallization history, at least for the V14 and V21 samples, i.e. precipitation from alcohol *versus* melt crystallization yields compositional differences (we surmise that the as-received V10 and V18 samples may have a similar history of precipitation from alcohol). The extent by which CR composition can be influenced by its chemical environment during crystallization is a topic for further investigation. Such a study should also be helpful in exploring the hypothesis that VOH-rich and E-rich segments have differential solubilities in certain solvents, thereby leading to compositional variations in the CR regions. The annealing, for example, of V18, results in a restoration of partitioning to values typical of melt crystallization; therefore, if the properties of the EVOH copolymers were to depend on the composition of the CR, one would have to be concerned about thermal cycling altering the properties.

## CONCLUSIONS

<sup>13</sup>C CP/MAS n.m.r. spectroscopic techniques are used to acquire spectra of a series of ethylene (E)/vinyl alcohol (VOH) copolymers, covering the range from 10 to 68 mol% VOH, and also of the two homopolymers. Based on differences in the proton rotating frame relaxation times,  $T_{1\rho}^H$ , characteristic of the crystalline and non-crystalline regions, spectra of each region are isolated. It is found that the composition of the crystalline phase is very close to stoichiometric. In the composition range from 0 to 20 mol% VOH, where the PE lattice dominates<sup>4</sup>, substitution of a hydroxyl group for a proton appears to be a minor perturbation, causing only a modest lattice expansion. In that sense the

hydroxyl group behaves like an interstitial defect. It is also shown that concurrent with the incorporation of OH 'defects' in the lattice, there is still a strong exclusion of short-chain branches from the crystalline regions, just as there is in LDPE. The topic of the possible partitioning of VOH-VOH sequences is also raised over the E-rich composition range where the polyethylene lattice is present. It is found that the methine resonances in the spectra of the crystalline regions of these materials possess an upfield wing whose fractional intensity is close to the mole fraction of VOH. This experimental result is consistent with incorporation into the crystalline regions of all VOH blocks according to statistical availability, provided that the published assignment scheme for the methine multiplets in the EVOH copolymers is correct.

E-rich copolymers that had been precipitated from alcohol show a modest preference for E-residues in the CR regions. It is hypothesized that this modest partitioning is a result of the lower solubility of E-rich *versus* VOH-rich segments in alcohol so that the E-rich segments are preferentially selected for crystal formation.

Finally, a few comments are made regarding the methine spectral region of the PVOH homopolymer. It is noted that the CP intensities in that region are affected by the presence of water; also, in PVOH, some water is necessary in order that the  $T_{1\rho}^H$  method for separating resonances of crystalline domains can be implemented. This 'crystalline' spectrum showed methine multiplets whose intensities closely approximated the actual triad tacticities. This has not been seen previously when the spectra of the crystalline regions has been obtained based on  $T_1^C$  differences. Thus, we simply open the question of whether this unique finding is a matter of different sample histories or a matter of contrasting methods. If it is the latter, we further suggest that such a difference could arise when a variability of motion is present in the crystalline phase of PVOH.

## REFERENCES

- 1 Bunn, C. W. and Peiser, H. S. *Nature (London)* 1947, **159**, 161
- 2 Bunn, C. W. *Nature (London)* 1947, **160**, 929
- 3 Bodily, D. and Wunderlich, B. *J. Polym. Sci. (A-2)* 1966, **4**, 25
- 4 Matsumoto, T., Nakamae, K., Ogoshi, N., Kawasoe, M. and Oka, H. *Kobunshi Kagaku* 1971, **28**, 610
- 5 Matsumoto, T., Nakamae, K., Oka, H., Kawai, S. and Ochiuni, T. *Sen-i Gakkaishi* 1975, **35**, T152
- 6 Nakamae, K., Kameyama, M. and Matsumoto, T. *Polym. Eng. Sci.* 1979, **19**, 572
- 7 Matsumoto, T., Nakamae, K., Oshiyuni, T., Kawai, S. and Shioyama, T. *Sen-i Gakkaishi* 1977, **33**, T49
- 8 Ramakrishnan, S. *Macromolecules* 1991, **24**, 3753
- 9 Ketels, H., de Haan, J., Aerdts, A. and van der Velden, G. *Polymer* 1990, **31**, 1420
- 10 VanderHart, D. L. and Pérez, E. *Macromolecules* 1986, **19**, 1902
- 11 Pérez, E. and VanderHart, D. L. *J. Polym. Sci. Polym. Phys. Edn* 1987, **25**, 1637
- 12 Crissman, J. M. *Polym. Eng. Sci.* 1991, **31**, 541
- 13 Dorman, D. E., Otacka, E. P. and Bovey, F. A. *Macromolecules* 1972, **5**, 574
- 14 Terao, T., Maeda, S. and Saika, A. *Macromolecules* 1983, **16**, 1535
- 15 Horii, F., Hu, S., Ito, T., Odani, H., Kitamaru, R., Matsuzawa, S. and Yamaura, K. *Polymer* 1992, **33**, 2299
- 16 Wagner, H. and McCrackin, F. L. *J. Appl. Polym. Sci.* 1977, **21**, 2833
- 17 Certain commercial companies and products are named in order

- to specify adequately the experimental procedure. This in no way implies endorsement or recommendation by NIST
- 18 Van Der Linden, R., Koopmans, R. J. and Vansant, E. F. *J. Adhes.* 1980, **11**, 191
- 19 Schaefer, J., Stejskal, E. O. and Buchdahl, R. *Macromolecules* 1975, **8**, 291
- 20 Abragam, A. 'Principles of Nuclear Magnetism', Oxford University Press, Oxford, 1961, Ch. 5, p. 136
- 21 VanderHart, D. L., Earl, W. L. and Garroway, A. N. *J. Magn. Reson.* 1981, **44**, 361
- 22 VanderHart, D. L. *J. Magn. Reson.* 1981, **44**, 117
- 23 Moritani, T. and Iwasaki, H. *Macromolecules* 1978, **11**, 1251.
- 24 Earl, W. L. and VanderHart, D. L. *Macromolecules* 1979, **12**, 762
- 25 Rulands, W. *Acta Crystallogr.* 1961, **14**, 1180
- 26 Koopmans, R. J., Van Der Linden, R. and Vansant, E. F. *Polym. Eng. Sci.* 1983, **23**, 306
- 27 VanderHart, D. L. and Khoury, F. *Polymer* 1984, **25**, 1589
- 28 Hu, S., Horii, F. and Odani, H. *Bull. Inst. Chem. Res. Kyoto Univ.* 1991, **69**, 165
- 29 Hu, S., Tsuji, M. and Horii, F. *Polymer* 1994, **35**, 2516
- 30 Shewmon, P. G. 'Diffusion in Solids', 2nd Edn, Minerals, Metals and Materials Society, Warrendale, PA, 1989
- 31 Pfeffer, P. E., Hicks, K. B., Frey, M. H., Opella, S. J. and Earl, W. L. *J. Carbohydr. Chem.* 1984, **3**, 197
- 32 Ketels, H., Beulen, J. and van der Velden, G. *Macromolecules* 1988, **21**, 2032
- 33 Frensdorff, H. K. *Macromolecules* 1971, **4**, 369
- 34 Flory, P. J. *Trans. Faraday Soc.* 1955, **51**, 848
- 35 Sanchez, I. C. and Eby, R. K. *J. Res. Natl Bur. Stand. Sect. A* 1973, **77**, 353